Computer-Aided Design 160 (2023) 103532

Contents lists available at ScienceDirect

Computer-Aided Design

journal homepage: www.elsevier.com/locate/cad

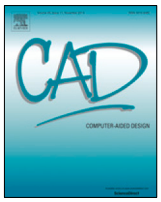

Interactive Structural Topology Optimization with Subjective Scoring and Drawing Systems

Zhi Li, Ting-Uei Lee, Yi Min Xie *

Center for Innovative Structures and Materials, School of Engineering, RMIT University, Melbourne, 3001, Australia

ARTICLE INFO

Article history:
Received 8 January 2023
Received in revised form 7 March 2023
Accepted 5 April 2023

Dataset link: https://doi.org/10.25439/rmt.22560256.v1

Keywords:
Topology optimization
Subjective preferences
Scoring
Drawing
Structural design

ABSTRACT

Topology optimization techniques can create efficient and innovative structural designs by redistributing underutilized materials to the most-needed locations. These techniques are typically performed based purely on structural performance without considering factors like aesthetics and other design requirements. Hence, the obtained structural designs may not be suitable for specific practical applications. This study presents a new topology optimization method, SP-BESO, by considering the subjective preferences (SP) of the designer. Here, subjective scoring and drawing systems are introduced into the popular bi-directional evolutionary structural optimization (BESO) technique. The proposed SP-BESO method allows users to iteratively and interactively create topologically different and structurally efficient solutions by explicitly scoring and drawing their subjective preferences. Hence, users do not need to passively accept the optimization results. A user-friendly digital design tool, iBESO, is developed, which contains four optimizers to simultaneously perform the proposed SP-BESO method to assist in the design exploration task. A variety of 2D examples are tested using the iBESO software to demonstrate the effectiveness of the proposed SP-BESO method. It is found that the combination of parameters used in the scoring and drawing systems controls the formation of final structural topologies toward performance-driven or preference-driven designs. The utilization of the proposed SP-BESO method in potential practical applications is also demonstrated.

1. Introduction

1.1. Background

Topology optimization is an effective strategy to create lightweight and high-performance structures by redistributing materials in continuous design domains [1,2]. In recent years, this technique has been utilized across a wide range of disciplines also due to its ability to design elegant and innovative structures, with applications including architectural designs [3–6], furniture [7,8], and additive manufacturing [9–12]. Conventional topology optimization techniques are performed based on finite element analysis (FEA). They typically require the continuous design domain to be discretized into finite element meshes to represent the given materials. One of the widely used topology optimization techniques is the bi-directional evolutionary structural optimization (BESO) method; it can redistribute the underutilized material to the most-needed locations by adding or removing the finite elements [13–16].

According to [17], the 'best design' generated from topology optimization based purely on structural performance may be of low value in practical applications, as it does not always satisfy all design requirements, including factors like aesthetics quality [18]. To overcome this bottleneck, recent research has extended the BESO method to generate multiple diverse solutions while maintaining a high level of structural efficiency, offering diverse 'options' for users to select. This is called multi-solution strategies [17] (see Section 1.3). Such strategies sacrifice a small amount of structural performance (e.g., 3% stiffness) of the best design in exchange for multiple solutions. They can be achieved by introducing randomness to disturb the optimization process [19–21], changing the optimization settings [6,14,22,23], and/or adding structural complexity control to modify optimal topologies [24–26].

Although multi-solution strategies can provide many design options, picking a satisfactory final design can be a difficult task. During the selection process, evaluating each design option is time-consuming, and solutions that meet all design requirements may be rare [27]. Hence, excessive design options can lead to a high cost in finding the final design. As discussed in [28], design exploration is an evolutionary process rather than picking an appropriate outcome from various options, meaning users should add their subjective considerations to guide the design process. Therefore, to generate a useful list of design options, users should

* Corresponding author.
E-mail address: mike.xie@rmit.edu.au (Y.M. Xie).

https://doi.org/10.1016/j.cad.2023.103532
0010-4485/

be allowed to subjectively engage in the optimization process [29,30].

It should be noted that different design tasks require different levels of subjective involvement, where low and high levels of involvement in structural design result in performance-driven and preference-driven designs, respectively [31,32]. Performance-driven designs do not require much subjective involvement, thus suitable for applications where structural performance is critical, such as bridge designs [33]. Although such designs can create high-performance configurations, designers typically fail to add their creative ideas to affect the formation process of the final outcomes, meaning the designers have to passively accept the optimal solution from optimization. On the other hand, preference-driven designs focus on creativity and aesthetics, and are less concerned about structural performance; therefore, the key geometric features of the final structural design can be fully controlled by subjective preferences, where optimization is utilized as a supporting role in design exploration [7].

Structural optimization methods considering subjective preferences can find a satisfying design more efficiently [34,35]. For example, [36] uses an evolutionary algorithm considering subjective preferences to create a variety of satisfying truss optimization results. This study is enlightening because it demonstrates the potential of achieving design objectives while considering subjective preferences using an optimization framework. Their method allows users iteratively and interactively to find the ideal solution, whether it is a performance-driven or preference-driven design. Besides, a recent survey has reported that manually applying subjective modifications to given optimal topologies based on aesthetic principles can result in more satisfying designs [18]. There is a huge potential to use topology optimization that considers subjective preferences to iteratively and interactively generate a wide variety of satisfying structural designs. However, it is an ongoing challenge and remains under-explored.

1.2. Scope of work

This paper proposes a new topology optimization method that considers subjective preferences, named 'SP-BESO'. The proposed method combines two subjective involvement approaches with the multi-solution optimization strategy. This combination enables users to iteratively and interactively create diverse, satisfying structural designs by explicitly scoring and drawing their subjective preferences. Section 2 gives details of the proposed SP-BESO method. Section 3 introduces a new digital design tool, 'iBESO', achieved using the SP-BESO method. Section 4 performs parametric investigations. Section 5 demonstrates two potential practical applications of the proposed SP-BESO method. Section 6 discusses possible extensions of the proposed SP-BESO method, followed by a conclusion in Section 7.

1.3. Key contributions

The proposed SP-BESO method converts subjective preferences into a list of weights in topology optimization through scoring or drawing in order to obtain topologically different and structurally efficient solutions. Note that SP-BESO is a new extension of the conventional BESO method [15]. There are a few extensions of the BESO method that share a similar goal, also aiming to obtain diverse and efficient structural designs considering subjective preferences. The key contributions of the SP-BESO and its differences from previous studies are summarized as follows.

First, [25,37] present three multi-solution BESO methods considering subjective interventions, including multi-radius BESO (MR-BESO), multi-volume BESO (MV-BESO), and multi-weight BESO (MW-BESO). MR-BESO and MV-BESO introduce different filter radius and volume constraints, respectively, in different regions of the continuous design domain [25]. Due to this, users need to adjust the optimization parameters at different regions based on local design requirements. Although such methods can create diverse solutions, setting many local optimization parameters may be tedious and time-consuming, and the results rely on a trial-and-error process to satisfy all design requirements, including subjective preferences. The proposed SP-BESO method uses a global filter radius and volume constraint to avoid these problems, with the weighting method used to straightforwardly involve subjective preferences. MW-BESO also uses the weighting method by introducing subjective drawn patterns [25,37]. However, in contrast to SP-BESO, MW-BESO is not yet an interactive topology optimization method, meaning users cannot further modify the results to achieve the 'most-desired' structural design through subsequent topology optimization.

Second, [26] explicitly prescribes the locations and number of holes in the BESO method to affect the formation of final structural topologies. Although the locations and number of holes can be prescribed based on subjective preferences, the final hole shapes are not controllable. Hence, the obtained solutions may not always satisfy all subjective design requirements. In SP-BESO, the number of holes and their locations and shapes can be considered subjective factors by the scoring or drawing systems, meaning the solutions can implicitly involve all subjective design requirements. The subsequent topology optimization can be used to improve the obtained solution through an evolutionary design exploration process.

Together, it can be understood that the proposed SP-BESO method can iteratively and interactively create diverse and efficient structural designs using subjective scoring or drawing systems. It offers a new evolutionary design exploration strategy to effectively achieve desired structural designs so that users do not need to passively accept the optimization results.

2. Structural topology optimization

In this study, the proposed structural topology optimization framework is developed based on the soft-kill BESO method [15], briefly summarized in Section 2.1. Three additional features are added to this framework, introduced in Sections 2.2–2.4. Together, a new topology optimization method considering subjective preferences, Subjective Preferences (SP)-BESO, is proposed in Section 2.5.

2.1. Soft-kill BESO method

This study uses the soft-kill BESO method to perform structural topology optimization. The stiffness maximization (compliance minimization) problem subject to a volume constraint can be formulated as follows:

$$min: \quad C = \frac{1}{2}\mathbf{U}^T\mathbf{K}\mathbf{U} \tag{1a}$$

$$s.t.: \quad V^* = \sum_{i=1}^{N} v_i \rho_i \tag{1b}$$

$$\rho_i = \rho_{min} \text{ or } 1 \tag{1c}$$

where compliance, C, is the inverse measure of structural stiffness; $\mathbf{U}$ and $\mathbf{K}$ are the global displacement vector and the global stiffness matrix, respectively; V^* and v_i are the target structural volume and the volume of ith element, respectively. Note that the given design domain is discretized into N elements, where each element, i, has a design variable, ρ_i, to determine whether the element is solid ($\rho_i = 1$) or void ($\rho_i = \rho_{min} = 0.001$).

To achieve a nearly solid–void design, the material model of structural elements is defined as a function of the element density:

$$E(\rho_i)^k = \rho_i^p E_0 \tag{2}$$

where $E(\rho_i)^k$ is Young's modulus of ith structural element at the kth iteration, E_0 is the design Young's modulus of structural elements, and $p = 3$ is the penalty exponent [2].

It should be noted that the soft-kill BESO method determines the topology according to the relative ranking of sensitivity numbers, α_i. The ith elemental sensitivity number is defined as:

$$\alpha_i = -\frac{1}{p}\frac{\partial C}{\partial x_i} = \begin{cases} \frac{1}{2}\mathbf{u}_i^T\mathbf{k}_i\mathbf{u}_i, & \text{when } \rho_i = 1 \\ \frac{\rho_{min}^{p-1}}{2}\mathbf{u}_i^T\mathbf{k}_i\mathbf{u}_i, & \text{when } \rho_i = \rho_{min} \end{cases} \tag{3}$$

where $\mathbf{k}_i$ is the elemental stiffness matrix and $\mathbf{u}_i$ is the elemental displacement vector.

To avoid checkerboard and mesh dependency problems, the following filtering operation is used to smooth the above raw sensitivity number [38]:

$$\tilde{\alpha}_i = \frac{\sum_{j=1}^{N}(r_{min} - r_{ij})\alpha_i}{\sum_{j=1}^{N}(r_{min} - r_{ij})} \tag{4}$$

where $\tilde{\alpha}_i$ is the filtered sensitivity number, r_{min} is the filter radius, and r_{ij} represents the distance between the centroids of elements i and j.

To improve the convergence of the BESO technique, the current and historical sensitivity numbers can be averaged using the following equation [15]:

$$\hat{\alpha}_i = \frac{\tilde{\alpha}_i^{\,k} + \tilde{\alpha}_i^{\,k-1}}{2} \tag{5}$$

where $\hat{\alpha}_i$ is the averaged sensitivity number.

In each iteration, structural elements are added or removed according to the sensitivity threshold procedure. The target volume for the next iteration, $\mathbf{V}^{k+1}$, needs to be given before elements are removed from or added to the current design:

$$\mathbf{V}^{k+1} = \mathbf{V}^k(1 \pm ER) \tag{6}$$

where $\mathbf{V}^k$ is the current volume and ER is the evolutionary volume ratio.

Next, the bisection method is used to add or remove elements based on $\hat{\alpha}_i$ [39]. The optimization process is repeated until the following convergence criteria are satisfied [14].

$$\frac{|\sum_{m=1}^{M}(C_{k-m+1} - C_{k-M-m+1})|}{\sum_{m=1}^{M} C_{k-m+1}} \leq \tau \tag{7}$$

where $M = 5$ is an integer number and $\tau = 0.001$ is the allowable convergence error. Here, M is set as 5, meaning stable compliance values are checked in the last 10 iterations.

2.2. Generation of multiple solutions

Conventional topology optimization methods can only generate one structural topology under the same settings. This study uses the random perturbations method [20] to allow the soft-kill BESO method to generate different competitive structural topologies every time, thereby providing multiple solutions.

To summarize, the random perturbations method introduces a random coefficient, β_i, to penalize α_i in each iteration:

$$\bar{\alpha}_i^{\,r} = \alpha_i\beta_i, \quad \beta_i \in [1-\epsilon, 1+\epsilon] \tag{8}$$

where $\bar{\alpha}_i^{\,r}$ is the penalized sensitivity number; ϵ determines the random range of β_i, which is set as $\epsilon = 0.15$ in this study. Note that all random coefficients are generated before the optimization process. Hence, the ranking of α_i is changed into $\bar{\alpha}_i^{\,r}$, which affects the selection of elements being added or removed in the threshold procedure, ultimately creating a different structural topology. Moreover, the generation of random coefficients is driven by the random seed integer, γ, where different γ can result in different sets of random coefficients. Due to this, infinite solutions can be obtained by modifying γ, thereby significantly improving the design diversity of topology optimization.

2.3. Subjective scoring

This study proposes a weight-based strategy to introduce subjective preferences into the method described in Section 2.2. The strategy quantifies preferences by explicitly scoring the existing optimization design ('parent design'). Then, the subjective score is used to generate weights in the next topology optimization to create new designs ('child design'). The child design can be used as an updated parent design in the subsequent topology optimization, resulting in a further improved child design. By alternately inputting subjective preferences and executing topology optimization, users can iteratively explore the desired design. Note that the subsequent topology optimization should start from the beginning based on the parameters of the parent design.

Here, the scoring weight, $\omega_i^{\,s}$, is used to penalize the elemental sensitivity number:

$$\omega_i^{\,s} = 1 + \lambda_s\rho_i\frac{S}{10}, \ \lambda_s \in [0, 1], \ S \in [-5, 5] \tag{9a}$$

$$\bar{\alpha}_i^{\,s} = \omega_i^{\,s}\alpha_i \tag{9b}$$

where $\bar{\alpha}_i^{\,s}$ is the modified sensitivity number of the ith element after scoring; λ_s is a parameter ranging from 0 to 1, which allows users to control the influence of scoring weights on topology optimization; S is the subjective score, which can be selected within a specific interval, e.g., $[-5, 5]$. Together, the default range of $\omega_i^{\,s}$ is [0.5, 1.5].

As shown in Fig. 1, applying a negative ($S = -2$) and positive ($S = 2$) subjective score on the same parent design (see Fig. 1(a)) gives different child designs. It should be noted that when $S < 0$, the parent design is considered an undesirable solution; when $S > 0$, the parent design is considered a preferred solution. In Fig. 1(b), as S is set to be -2, the modified sensitivity numbers at solid regions are lower than void regions. Hence, the subsequent topology optimization will avoid producing a similar solution to the parent design, leading to a new design that may help users to find their desired solutions, as shown in Fig. 1(c). In Fig. 1(d), as S is set to be 2, the modified sensitivity numbers at solid regions are higher than the void regions. In that case, the child design will only be slightly different from its parent design, as shown in Fig. 1(e). Note that using $S = 0$ will not change the parent design in the subsequent topology optimization.

2.4. Subjective drawing

Another strategy to include subjective preferences in topology optimization is to employ 'hand-drawn patterns', where drawing allows users to put their creative ideas into structural designs based on their artistic intuition [40]. It is worth pointing out that it is difficult for users who lack experience in structural design to produce high-performance structure sketches that will fulfill all design requirements. Due to this, this study converts the given drawn pattern to a list of 'drawing weights' to modify the elemental sensitivity numbers, thereby guiding the topology optimization process to achieve suitable designs considering both structural performance and subjective preferences.

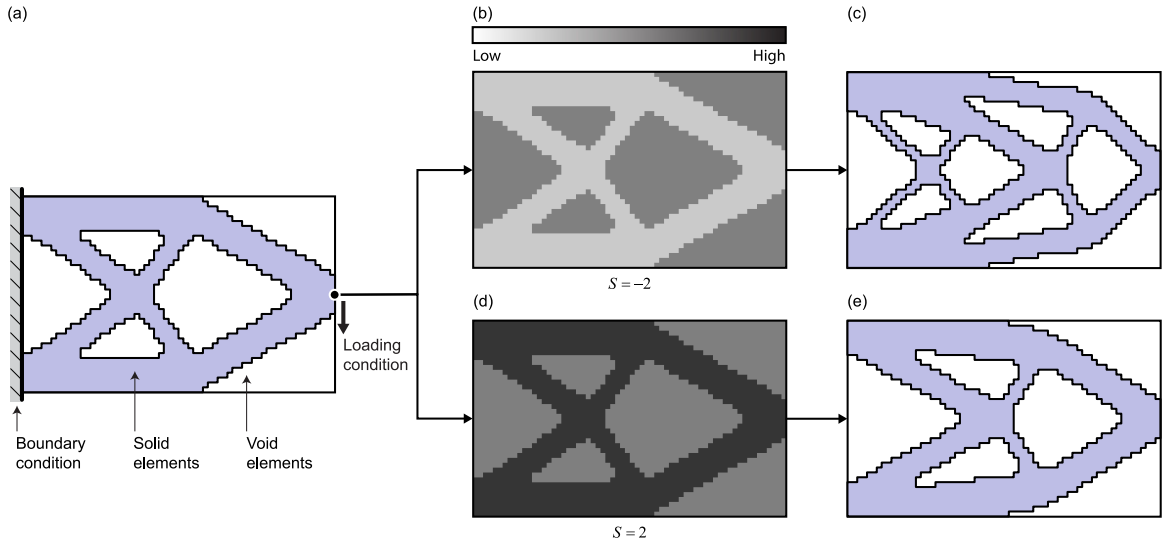

Fig. 1. Applying subjective scores in topology optimization: (a) parent design; (b) visualization of applying $S = -2$ on the parent design; (c) child design obtained using $S = -2$; (d) visualization of applying $S = 2$ on the parent design; (e) child design obtained using $S = 2$. (For interpretation of the references to color in this figure legend, the reader is referred to the web version of this article.)

In this study, a drawn pattern is first translated to a grayscale raster texture made up of pixels. Next, the colors of pixels are used to calculate the drawing weights. Note that the color scale ranges from black through gray to white.

For simplicity, the normalized elemental sensitivity number, ${\omega_i}^e$, is used:

$$ {\omega_i}^e = \frac{\alpha_i - \alpha_{min}}{\alpha_{max} - \alpha_{min}} \tag{10} $$

where α_{min} and α_{max} represent the minimum and maximum raw sensitivity numbers, respectively.

Here, the drawing weight, ${\omega_i}^d$, and the modified sensitivity number considering the drawn pattern, ${\bar{\alpha}_i}^d$, are calculated using:

$$ {\omega_i}^d = \frac{\sum_{j=1}^{D}(1 - c_j)}{D}, \ c_j \in [0, 1] \tag{11a} $$

$$ {\bar{\alpha}_i}^d = \lambda_e {\omega_i}^e + \lambda_d {\omega_i}^d, \ \lambda_e, \lambda_d \in [0, 1] \tag{11b} $$

where D is the number of nodes in the ith element; c_j is the gray color of the jth node on the texture, ranging from 0 (black) to 1 (white); λ_d and λ_e are parameters within [0, 1], which control the influence of ${\omega_i}^d$ and ${\omega_i}^e$, respectively. Note that controlling λ_d and λ_e allows users to balance objective structural performance with subjective artistic intuition according to design requirements, discussed later in Section 4.4.

For a given design domain (see Fig. 2(a)), drawing operations in topology optimization can be performed without or with a parent design. Fig. 2(b) shows the workflow of drawing without using a parent design, requiring users to draw a pattern based on their rough idea beforehand. The pattern is first converted into a weighted texture so that each element can obtain a drawing weight based on the color of the corresponding pixel. Using weighted texture, the formation of the final structural topology is affected by the drawn pattern, thereby generating a new design considering both structural performance and subjective preferences. Fig. 2(c) shows the workflow of drawing using a parent design, allowing users to make further modifications, such as adding new structural members. To achieve this, the nodal sensitivity field of the parent topology is first converted to a texture using the bilinear interpolation method [41]. Next, users can draw on the texture according to their subjective preferences. Finally, the subsequent topology optimization is performed to produce a child design considering the drawn pattern (i.e., the modified parent design).

2.5. SP-BESO method

The SP-BESO method is proposed here based on the combination of the multi-solution strategy (see Section 2.1), subjective scoring (see Section 2.2), and subjective drawing (see Section 2.3). To be specific, the elemental sensitivity number used in the SP-BESO method before filtering (see Eq. (4)), $\tilde{\alpha}_i$, is obtained by combining Eqs. (8), (9)(b) and (11)(b):

$$ \tilde{\alpha}_i = \beta_i {\omega_i}^s (\lambda_e {\omega_i}^e + \lambda_d {\omega_i}^d), \ \lambda_e, \lambda_d \in [0, 1] \tag{12} $$

The computational workflow of the proposed SP-BESO method is summarized in Fig. 3. It should be noted that the SP-BESO method is modified from the soft-kill BESO method. The new features are highlighted in this workflow, including the use of random penalty coefficients (green) and subjective weights (red). It is worth noting that the proposed SP-BESO method does not increase the algorithmic complexity of the underlying BESO method due to the use of the weighting method. Hence, the SP-BESO method requires almost the same computational resource consumption as BESO. The iteration numbers to generate a converged solution of SP-BESO can be found in Figs. 8(c) and 9(d); the actual run time depends on the complexity of the structural optimization problem and the hardware used.

3. iBESO digital design tool

3.1. iBESO overview

To further explore the capability of the proposed SP-BESO method, a user-friendly digital design tool, iBESO, is developed. The iBESO software has three unique systems: the multi-solution system, the scoring system, and the drawing system. These systems are detailed in the following subsections. The download link and the user guide of the iBESO software are available in [42].

The iBESO software can simultaneously perform up to four 2D topology optimization solvers based on the SP-BESO method, as shown in Fig. 4. This allows four parent designs to be parallel evaluated and further modified based on subjective preferences (scoring and drawing), resulting in child designs through subsequent topology optimization. The evaluation and modification processes can be repeated until an ideal structural design is obtained.

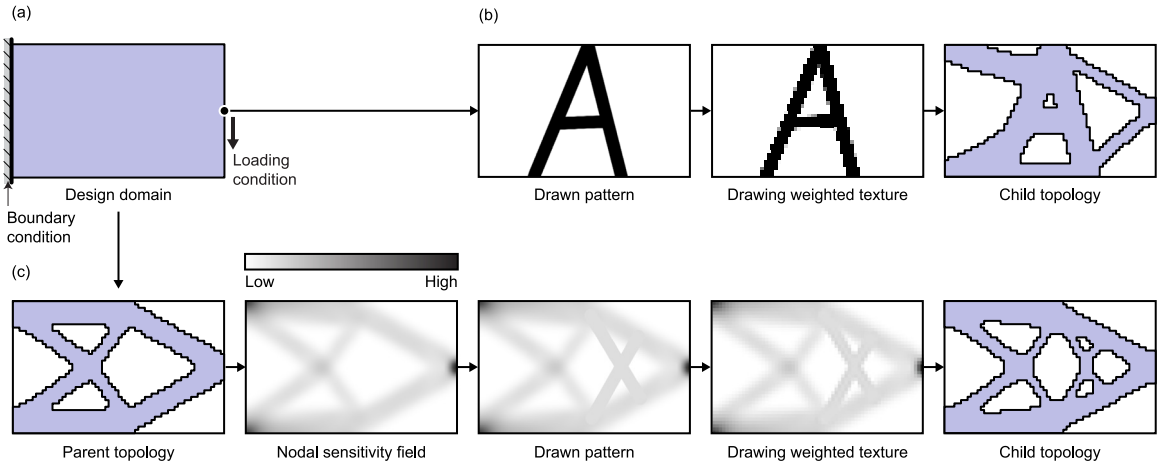

Fig. 2. Applying subjective drawing patterns in topology optimization: (a) optimization problem; (b) generating a child design using a prescribed pattern (letter 'A') without a parent design; (c) generating a child design by adding new members in the parent design. (For interpretation of the references to color in this figure legend, the reader is referred to the web version of this article.)

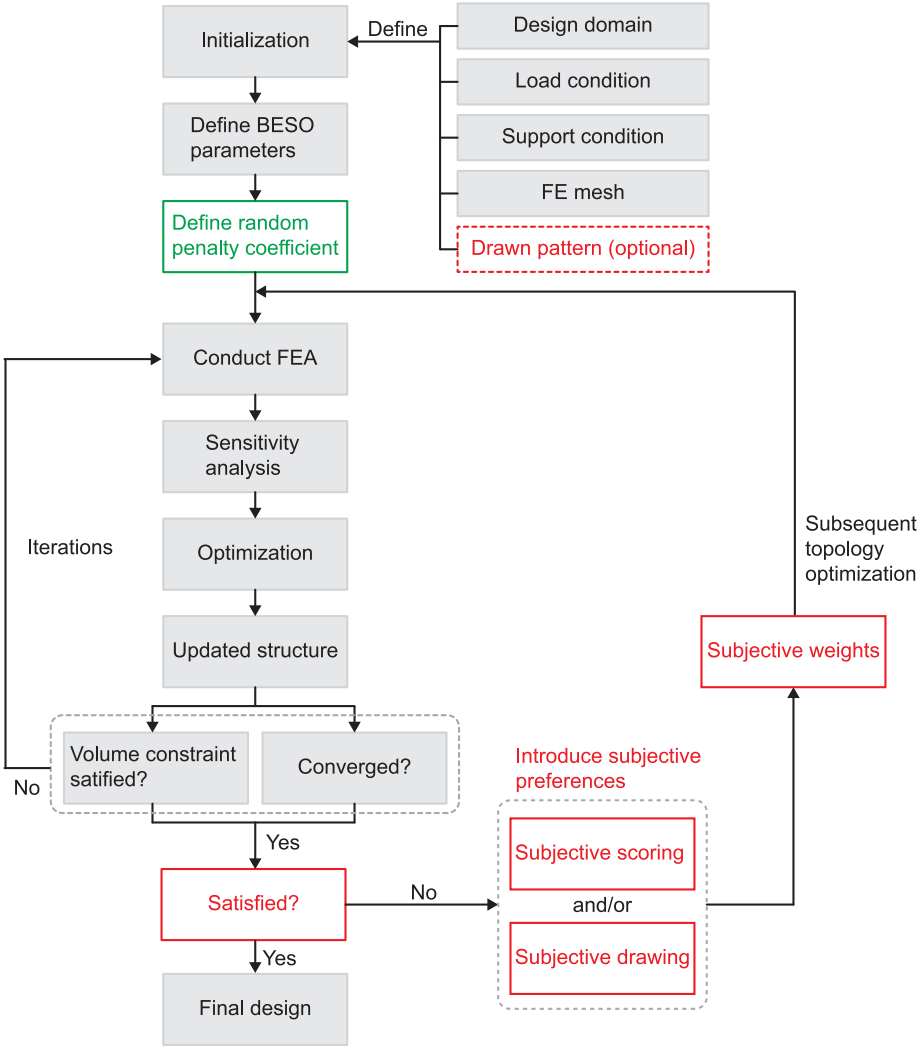

Fig. 3. Computational workflow of the proposed SP-BESO method. Note that the SP-BESO method is modified from the soft-kill BESO method. The two new features are highlighted in green and red. (For interpretation of the references to color in this figure legend, the reader is referred to the web version of this article.)

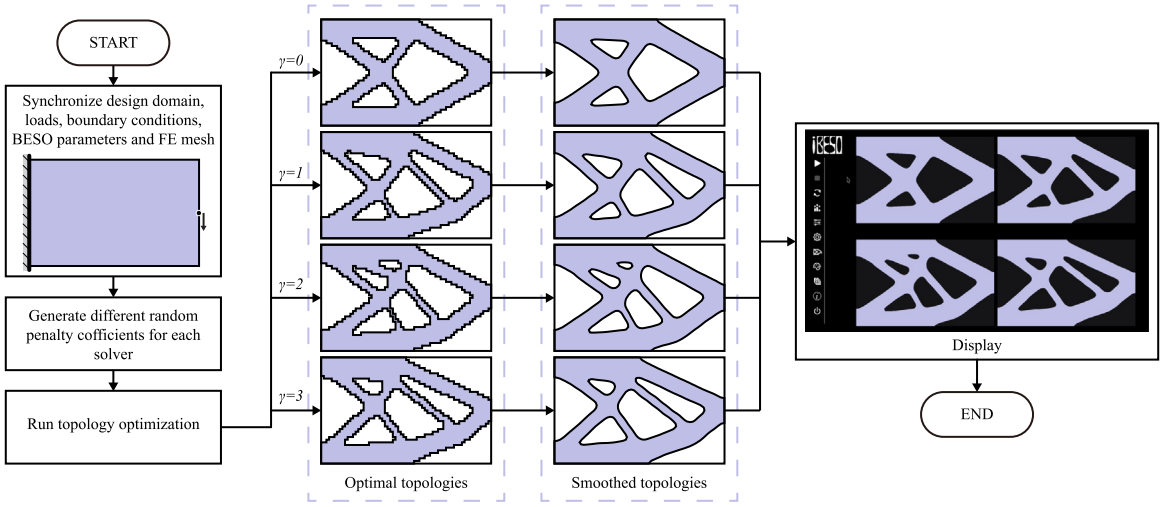

Fig. 4. Computational workflow of the multi-solution system in the iBESO software.

The implementation of iBESO is achieved using both C++ and C# programming languages. The C++ part contributes an efficient optimization kernel, which is modified from existing optimization codes [39,43,44]. The C# part gives the graphical user interface, allowing users to define boundary conditions and other design parameters explicitly and interactively.

3.2. Multi-solution system

The multi-solution system allows iBESO to create diverse, unexpected, and competitive designs. To avoid the over-choice problem, the iBESO software uses only four optimization solvers (expansion can be easily made). Thus, the number of solutions in every subsequent topology optimization is always four. As there is no limitation on the number of subsequent topology optimization that iBESO can perform, there could be infinite child designs. However, these child designs are considered useful, as they are generated using subjective preferences while maintaining high structural efficiency.

Fig. 4 summarizes the computational workflow of the multi-solution system in iBESO. Initially, the key difference between the four solvers is the use of different γ, leading to different random coefficients. It should be noted that β_i is set to be 1 when $\gamma = 0$. In that case, the solver will not be affected by random penalty coefficients, referring to the standard soft-kill BESO procedure (see Section 2.1). During optimization, the four solvers will start synchronously until all convergence conditions are satisfied. After optimization, zig-zag boundaries of the results are smoothed using the method proposed previously by the authors [45], enabling volumetric constraints and geometric features to be preserved. Note that the smoothed results may have slightly different structural performances, but they are only used for visualization purposes [45].

3.3. Scoring system

In iBESO, the scoring system is available after the four initial parent designs are obtained. The scoring system is demonstrated more clearly in Fig. 5. In every subsequent topology optimization, the four inputs (left) are treated as new parent designs with their design variables, ρ_i, recorded. Next, a scoring panel can be accessed for interactive evaluation to include subjective preferences. The specified S values are then used to calculate the scoring weights and determine the relative ranking of modified sensitivity numbers. Finally, the four optimization solvers are restarted to generate new child designs (right).

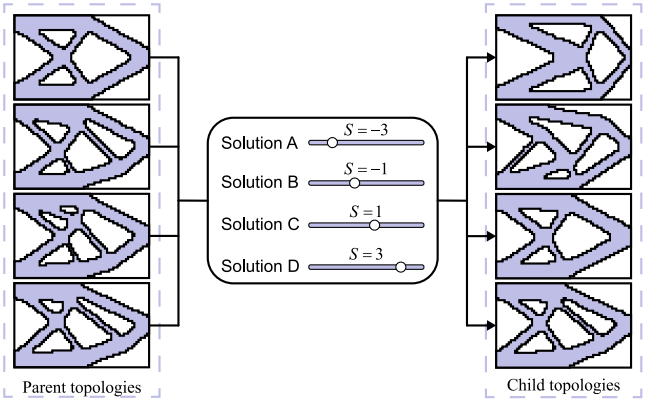

Fig. 5. Demonstration of the scoring system in the iBESO software.

3.4. Drawing system

In contrast to the scoring system, the drawing system can be activated before or after the first topology optimization process (see Section 2.4); both start with a user-defined grayscale texture drawn within the design domain. In iBESO, users can input their creative patterns by drawing manually or importing external grayscale raster images to all four solvers. These patterns are converted to drawing weights using Eqs. 11(a) and (b) to affect the subsequent topology optimization. When drawing inside the solvers, iBESO has a 'brush' tool (see Appendix), which allows users to draw grayscale patterns by stamping and swiping [46]. When importing from external images, iBESO can map 2D images with different sizes and resolutions to the prescribed design domain.

3.5. iBESO demonstration

Fig. 6 shows the initial interface of the iBESO software and the sub-interfaces after clicking the six major function buttons. It can be seen that the initial interface has four optimization solvers (dark rectangular areas) and a vertical toolbar. The toolbar includes 'Run', 'Stop', and 'Reset' buttons to control the optimization process of the four solvers; a 'Quit' button is also included to shut the iBESO software. Other buttons in the toolbar control the six major functions of the iBESO software, which will open sub-panels:

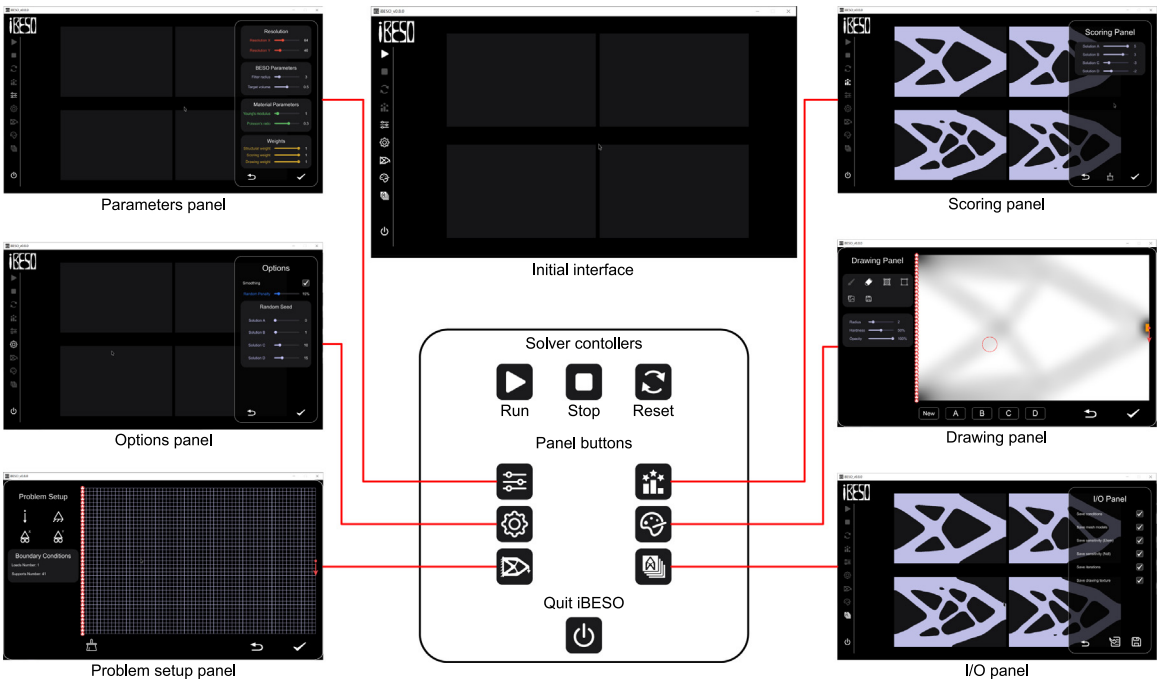

Fig. 6. Demonstration of the initial interface of the iBESO software and the sub-interfaces after clicking the six major function buttons.

- Parameters panel: It controls the design resolution (number of elements in the X and Y directions), BESO parameters (filter radius r_{min} and target volume fraction V^*), materials parameters (Young's modulus E_0 and Poisson's ratio ν), and the subjective parameters (λ_e, λ_s, and λ_d).
- Options panel: It allows users to choose whether to smooth solutions and control the random seed parameters for the four solvers.
- Problem setup panel: It allows users to add, remove, and modify load and support conditions graphically by clicking the selected nodes.
- Scoring panel: It can be opened after the four solvers have converged. Four sliders are used to give scores on the current optimization results.
- Drawing panel: Users can draw their creative patterns by clicking or dragging the mouse. The buttons on the left include 'drawing', 'erasing', 'drawing passive solid domains', 'drawing passive void domains', 'importing a texture', and 'exporting the current texture'. Note that 'passive' elements will not change their design variables during optimization. Besides, three sliders are included to control the size, hardness, and opacity of the brush (see Appendix)
- Input/Output (I/O) panel: It allows users to export the current four solutions or import a structural design problem and parameters.

4. Parametric investigations

4.1. Measuring method

Parametric investigations (see Sections 4.3–4.4) are conducted using the iBESO software. In order to thoroughly compare two given structural topologies (denoted here as solutions A and B), three metrics are used to quantify the differences in shape and structural performance.

First, the difference in structural performance can be represented by the compliance ratio, $\Delta C = C_B/C_A$, where C_A and C_B are the compliance of solutions A and B, respectively. According to [20,21,25,26], this is the most straightforward method to evaluate the difference between two topology optimization methods under the same settings.

Second, the overlapping rate P can be used to measure the similarity of the two solutions [23], as shown in Fig. 7. The overlapping rate can be calculated by:

$$P = \frac{V_P}{V^*} \tag{13}$$

where V_P is the volume fraction of the overlapping part. For example, comparing Figs. 7(a) with (b) gives $P = 88.97\%$, representing the percentage of the overlapping area of the two structural topologies. Note that P is a simple and effective measure for comparing BESO-based results, as it compares the shape of two structural topologies based on overlapping solid elements only. Other methods, such as DCC, DMCC, and DSSD, can also measure the differences between two structural topologies, but they require more complex calculations, which is unnecessary for this study. Details of DCC, DMCC, and DSSD can be found in [23,47].

It should be noted that P alone is insufficient to fully show the geometric difference between the two solutions. Hence, the third proposed metric measures the difference in the number of holes of two structural topologies, Δg. The number of holes, g, is closely related to the structural complexity, which has been widely adopted in previous studies [24,26,48,49]. Structures with many holes are typically considered complex and difficult to manufacture. However, some users treat complexity as a valuable aesthetic contribution [26]. Note that, in this study, g is only a part of many implicit subjective factors, meaning minimization of Δg is not a strict design objective. Specifically, Δg is only used to assist in measuring the similarity between two shapes, which must be used together with P. Mathematically, g can be calculated based on geometric information [50,51]:

$$2 - 2g = M_V - M_E + M_F \tag{14}$$

where M_V, M_E, and M_F represent the number of vertices, edges, and faces of the final FE mesh, respectively. For example, in Fig. 7,

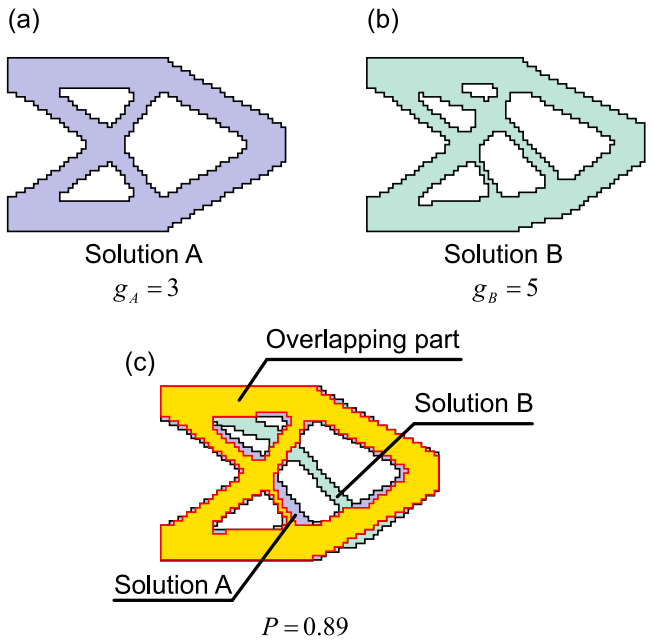

Fig. 7. Measuring of similarity between two structural topologies: (a) solution A with $g_A = 3$ holes; (b) solution B with $g_B = 5$ holes; (c) comparing solutions A and B gives the overlapping part. (For interpretation of the references to color in this figure legend, the reader is referred to the web version of this article.)

$\Delta g = g_B - g_A = 5 - 3 = 2$ represents the difference in the number of holes of solutions A and B.

In the following parametric investigations, solutions A and B are considered 'highly similar' when $\Delta C \approx 1$, $P \approx 1$, and $\Delta g \approx 0$.

4.2. Design parameters

The optimization problem used here is the classic 2D short cantilever example. An 80 mm tall × 50 mm wide design domain is first discretized into 4000 square elements that have a side length of 1 mm. A $F = -1$ N point load is applied at the center of the free edge, and the opposite edge is assigned with a fixed boundary condition. The material is assumed to be isotropic and linearly elastic, with Young's modulus of $E = 1$ MPa and Poisson's ratio of $\nu = 0.3$. BESO parameters are: $ER = 2\%$, $V^* = 50\%$, and $r_{min} = 3$ mm. Note that, to perform fair comparisons, all random penalty coefficients are set to 1 when generating the parent designs in Sections 4.3–4.4, meaning the optimization results are not disturbed by random perturbations.

In Section 4.3, the influence of scoring weights on optimization results is examined by setting different combinations of λ_s and S. The optimization process is performed on the same parent design (see Fig. 8(a)) with $\lambda_s = 0.1$, 0.5 and 1 tested, where S is set to be -3, -1, 1, and 3 to obtain solutions A–D in each test, respectively. Hence, 12 child designs (see Fig. 8(b)) are created. They are then compared with their parent design using the proposed metrics. Note that to avoid the interference of the drawing system, $\lambda_d = 0$ and $\lambda_e = 1$ are used.

In Section 4.4, the optimization problem is imparted with a drawn pattern, as shown in Fig. 9(a). Five child designs are created using different combinations of (λ_d, λ_e), including $(0.1, 1)$, $(0.1, 0.5)$, $(1, 1)$, $(0.5, 0.1)$, and $(1, 0.1)$. These child designs are compared with two reference designs, as shown in Fig. 9(b). The first reference is the BESO result obtained without activating the drawn pattern ($\lambda_d = 0, \lambda_e = 1$), and the second reference is the drawn pattern re-designed using topology optimization to achieve the target volume ($\lambda_d = 1, \lambda_e = 0$).

4.3. Results of using variable scoring weights

Figs. 8(b) and (c) show the results (structural topologies and evolution histories) of setting λ_s and S as design variables. First, it can be clearly seen that solutions A and B with disliked scores ($S < 0$) have different shapes to their parent design. To be specific, the overlapping rate P are all less than 90%, where the lowest case (solution A with $\lambda_s = 1$) has $P \approx 50\%$. Besides, most Δg values are not 0, where several low cases have $\Delta g = -5$. Note that the creation of different shapes is attributed to mutations (i.e., drastic changes in the structural topology, such as rod breakage) that occurred during the optimization (see spikes in the evolution histories). In contrast, solutions C and D with preferred scores ($S > 0$) have similar shapes to their parent design. Their P are relatively high, ranging from 89% to 98%, and with Δg to be either 0 or -2. It should be noted that solutions C and D are obtained from stable evolution histories, meaning the evolution histories do not have mutations; $\Delta g = -2$ is due to the two initially tiny holes being removed in the final topologies.

Moreover, it is seen that increasing λ_s can enhance the influence of scoring weights. For example, in solution A ($S < 0$), $P = 80\%$ when $\lambda_s = 0.1$, but P is reduced dramatically to 55.6% when $\lambda_s = 1$. However, for cases with $S > 0$, either high or low λ_s can make the subsequent child design close to the parent design, corresponding to a higher P, as they are preferred solutions already. In terms of structural performance, there is just a little difference between these 12 solutions. Only solution A with $\lambda_s = 1$ has a maximum ΔC of 1.038. Other designs have performance variations within 2% (i.e., $\Delta C < 1.02$).

Together, it can be concluded that both λ_s and S can control the formation of final topologies, and the effect of introducing scoring weights is in line with the expectation, which can provide competitive designs considering subjective scoring preferences.

4.4. Results of using variable drawing weights

Fig. 9(c) shows the five child designs obtained using a drawn pattern and different combinations of (λ_d, λ_e). Their evolutionary histories are given in Fig. 9(d). Detail comparisons with the two reference designs (see Fig. 9(b)) are summarized in Figs. 9(e)–(f) and Table 1. Note that the two references are extremely performance-driven (reference 1) and preference-driven designs (reference 2).

Here, different combinations of (λ_d, λ_e) are represented as $\Delta\lambda = \lambda_d - \lambda_e$. When $\Delta\lambda$ is increased from -0.9 to 0.9, it can be clearly seen that trends P_1 (P of reference 1) and P_2 (P of reference 2) decrease and increase, respectively (see Fig. 9(e)). This indicates that $\Delta\lambda$ plays an important role in determining the child designs to be performance-driven or preference-driven. Specifically, based on the shape comparison, when $\Delta\lambda$ is low (e.g., -1), $P_1 < P_2$, a performance-driven design is created; when $\Delta\lambda$ is high (e.g., 1), $P_1 > P_2$, a preference-driven design is created.

Fig. 9(f) shows the comparison of structural performance. In this figure, $\Delta C_1 \approx 1$ (ΔC of reference 1) represents a performance-driven design, which can be achieved using a low $\Delta\lambda$; $\Delta C_2 \approx 1$ (ΔC of reference 2) represents a preference-driven design, which can be achieved using a high $\Delta\lambda$. Both trends ΔC_1 and ΔC_2 are always increasing due to an increasing $\Delta\lambda$, representing a performance loss. Specifically, with increasing $\Delta\lambda$, trend ΔC_1 has increased away from $\Delta C = 1$, meaning the shape difference between the child design and the extreme performance-driven design is becoming larger, and trend ΔC_2 is increased toward $\Delta C = 1$, meaning the obtained child design is becoming more alike to the extreme preference-driven design. Note that the drawn pattern is specified based on artistic intuition only without considering the 'best' structural performance. Thus,

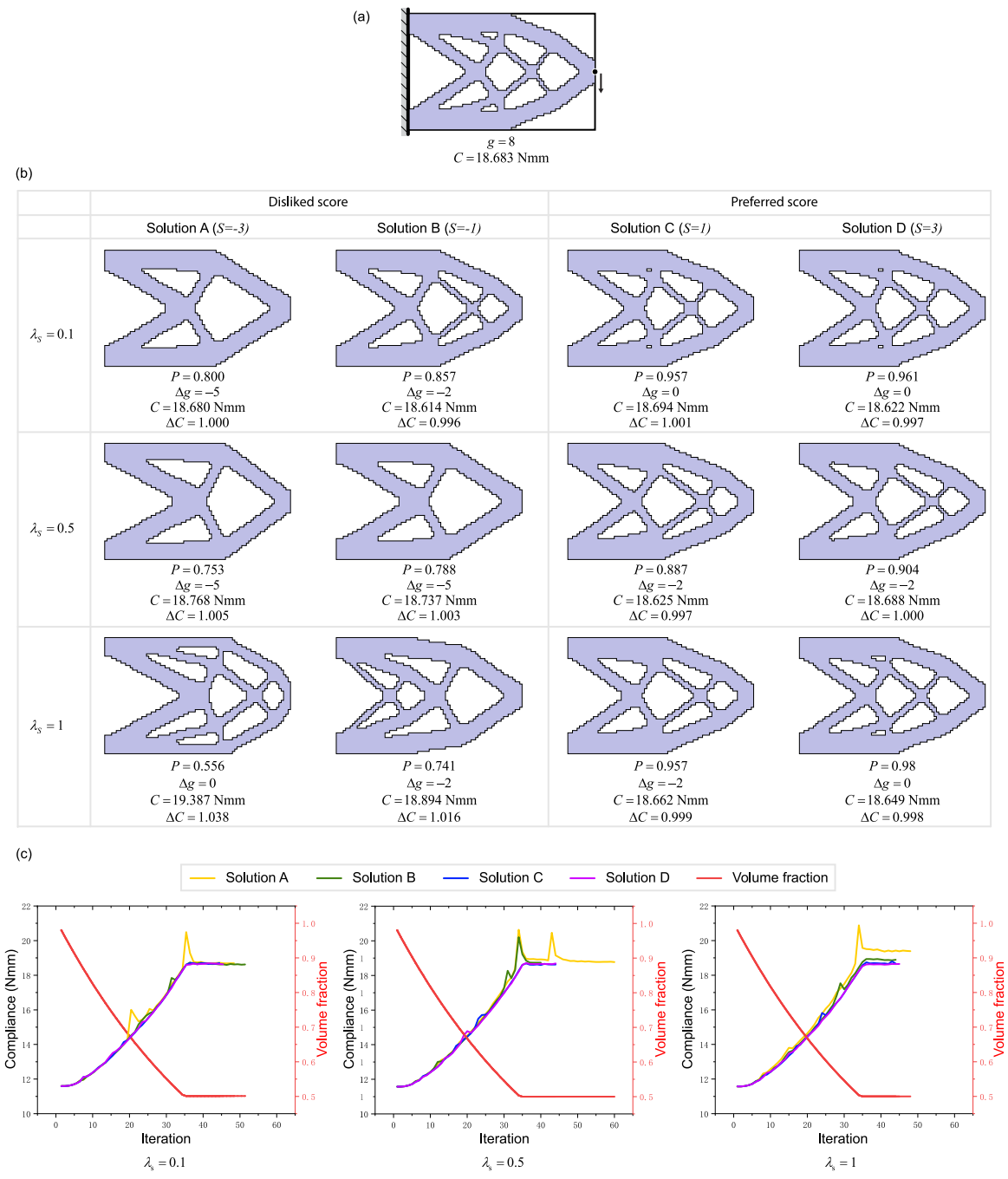

Fig. 8. Examining the influence of scoring weights on optimization results using the 2D short cantilever example: (a) the parent design and its loading and boundary conditions; (b) 12 child designs generated using three different λ_s (0.1, 0.5, and 1) and four different S (−3, −1, 1, 3); (c) comparison of evolutionary histories. (For interpretation of the references to color in this figure legend, the reader is referred to the web version of this article.)

the formation of the structural topology considering the drawn pattern is always guided away from the best performance-driven one, thereby introducing performance loss.

Together, it can be understood that using smaller $\Delta\lambda$ can result in the child designs closer to reference 1 (performance-driven), and higher $\Delta\lambda$ gives child designs closer to reference 2 (preference-driven). Although performance loss may be unavoided using a drawn pattern in topology optimization, the generated child designs have the potential to meet multiple design requirements and give unexpected shapes to inspire users to further improve the structural design.

5. Practical applications

Section 5 demonstrates the potential practical applications of the SP-BESO method in structural designs considering combined subjective scoring and drawing preferences; all results are obtained using the iBESO software and performed by the authors.

5.1. Bridge design

The first example is a simple 2D bridge, as shown in Fig. 10. The size of bridge is designed to be 240 mm wide and 80 mm

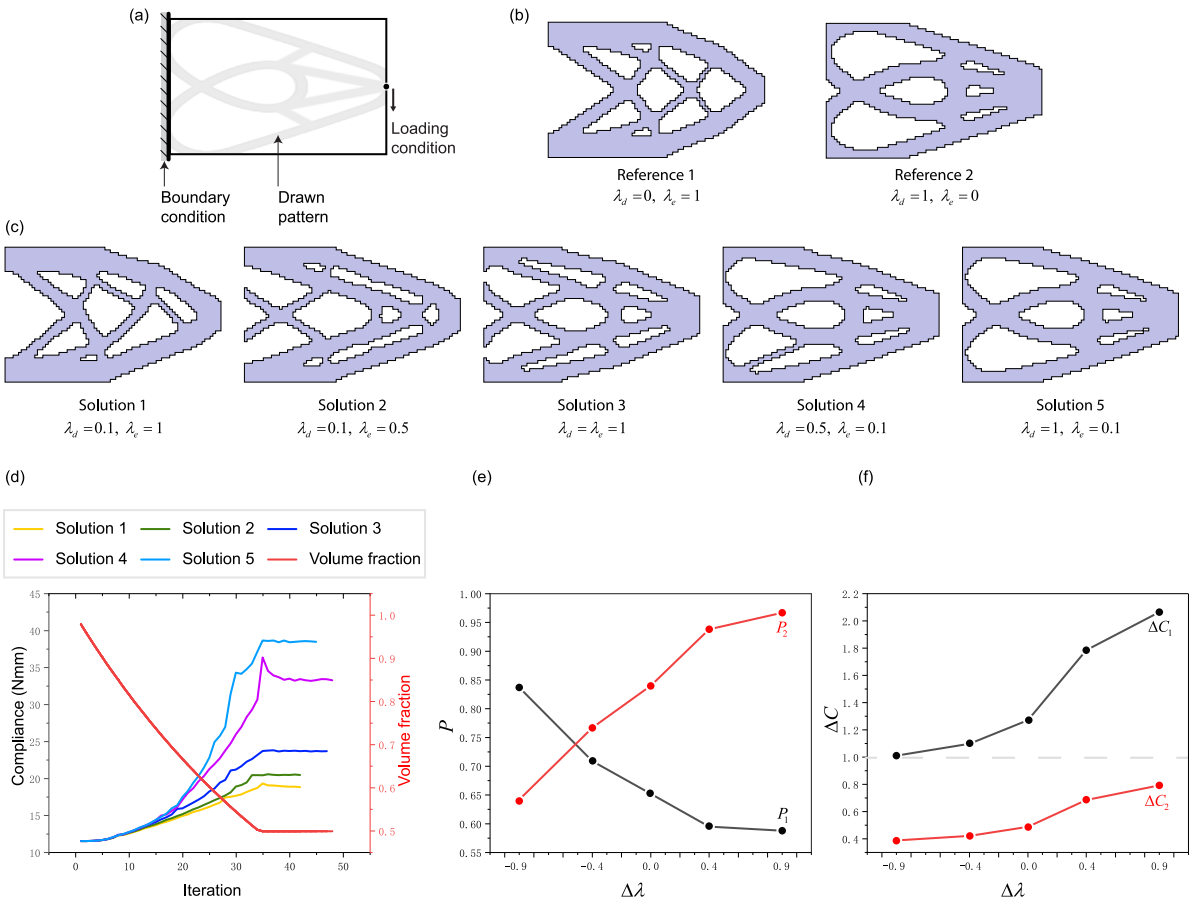

Fig. 9. Examining the influence of drawing weights on optimization results using the 2D short cantilever example: (a) the drawn pattern and its loading and boundary conditions; (b) left and right images are extreme performance-driven (reference 1) and preference-driven (reference 2) designs, respectively; (c) five child designs obtained using different combinations of λ_d and λ_e; (d) evolutionary histories; (e) comparison of P_1 and P_2 at different $\Delta\lambda$; (f) comparison of ΔC_1 and ΔC_2 at different $\Delta\lambda$. (For interpretation of the references to color in this figure legend, the reader is referred to the web version of this article.)

Table 1
Detail comparisons of the child designs (solutions 1–5) with the two reference designs. ΔC_1, P_1 and Δg_1 are the comparison data with reference 1; ΔC_2, P_2 and Δg_2 are the comparison data with reference 2.

Design	$\Delta\lambda$	C (N mm)	ΔC_1	ΔC_2	P_1	P_2	g	Δg_1	Δg_2
Reference 1	−1	18.683	–	–	–	–	8	–	–
Reference 2	1	48.674	–	–	–	–	6	–	–
Solution 1	−0.9	18.886	1.011	0.388	0.837	0.645	7	−1	1
Solution 2	−0.4	20.518	1.098	0.422	0.709	0.767	7	−1	1
Solution 3	0	23.749	1.271	0.488	0.652	0.840	6	−2	0
Solution 4	0.4	33.342	1.785	0.685	0.595	0.938	7	−1	1
Solution 5	0.9	38.560	2.064	0.792	0.588	0.967	6	−2	0

tall. Due to symmetry, only half of the structure needs to be modeled. The bridge deck is defined as the passive (non-design) solid domain subjected to a vertical uniformly distributed load with a total magnitude of 240 N [52]. Two points are set as fixed supports at the bottom of the design domain. BESO parameters are: $ER = 3\%$, $V^* = 25\%$, and $r_{min} = 3$ mm. Here, the subjective selection criteria are to achieve as many holes in the structural topology as possible, meaning child designs with higher g are preferred. It is also desirable to obtain a final design that is performance-driven but includes subjective considerations [33]. Due to this, only 15% of performance loss to the reference design (see Fig. 10(a)) is allowed; child designs with $\Delta C > 1.15$ are not accepted. Note that the reference design is obtained using the standard soft-kill BESO method described in Section 2.1, with $\gamma = 0$.

In Fig. 10(a), the four parent designs are obtained using $\lambda_e = 1$, $\lambda_s = 0$, and $\lambda_d = 0$, which indicate that the scoring and drawing systems are not yet considered. Among these four designs, solutions A and B have $g = 11$, greater than $g = 7$ (solution C) and $g = 9$ (solution D). Hence, they are short-listed as preferred candidates to perform subsequent topology optimization; solutions A–B are scored with $S = 4, 4, -4$, and -1, respectively.

Fig. 10(b) gives the four child designs obtained using $\lambda_e = 1$, $\lambda_s = 1$, and $\lambda_d = 0$, meaning the subjective scores of their parent designs are activated. Interestingly, these four child designs all have $g = 11$ and are considered competitive designs in terms of structural performance, where all ΔC are within [1.00, 1.04]. Comparing these four child designs, it can be seen that their hole arrangements are different, where the holes of solutions A–C are arranged as 3-5-3 (bottom-top-bottom), and solution D has 4-3-4. If one wishes to design the bridge with more holes near the supports, solution D may be preferred. It should be noted that

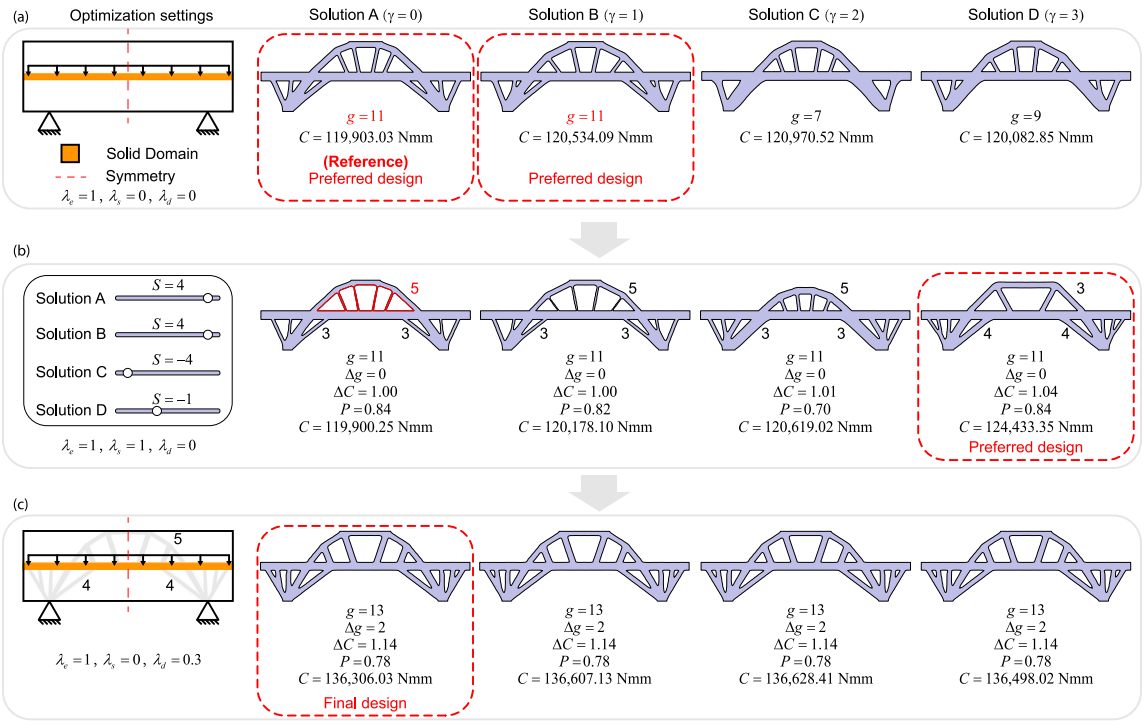

Fig. 10. 2D bridge design example using the proposed SP-BESO method. It is here desirable to achieve a final design that is performance-driven but possesses many holes: (a) parent designs; (b) child designs obtained considering the scores of their parent designs; (c) child designs obtained using the drawing system. (For interpretation of the references to color in this figure legend, the reader is referred to the web version of this article.)

solution D can be further modified using the proposed drawing system to achieve a more satisfying design.

As shown in Fig. 10(c), a manually drawn texture is used to generate a new generation of child designs, where $\lambda_e = 1$, $\lambda_s = 0$, and $\lambda_d = 0.3$. It should be noted that the drawn texture is mimicked from solution D of Fig. 10(b) but with two extra holes added to the top part of the bridge; the 13 holes are arranged as 4-5-4. It can be seen that the new child designs (see Fig. 10(c)) have a highly similar shape and structural performance, as all $g = 13$, $P = 0.78$, and $\Delta C = 1.14$. Here, solution A is selected as the final design, as it has the best structural performance ($C = 136,306.03$ N mm).

5.2. Chair design

The final example is a 2D chair, as shown in Fig. 11. The design domain of the chair is designed to be 80 mm deep and 80 mm tall. The seat and backrest parts are set as a continuous passive solid domain subjected to a uniform load of 1 N/mm [52]. Two points are fixed at the bottom of the design domain. Moreover, a passive void domain is added along the passive solid domain to avoid materials added in the seat and backrest areas during optimization. BESO parameters are: $ER = 3\%$, $V^* = 20\%$, and $r_{min} = 3$ mm. Here, the task is to create a list of competitive, preference-driven design options. The proposed subjective drawing system is used to assist the design exploration process.

Fig. 11(a) shows three reference designs obtained without using subsequent topology optimization. In detail, reference 1 is obtained using the standard soft-kill BESO method, and references 2–3 are obtained using different drawn patterns in SP-BESO with $\lambda_e = 0$, $\lambda_s = 0$, and $\lambda_d = 1$. References 2 is a curved chair, where the drawn pattern is inspired by the wiggle side-chair designed by the famous architect Frank Gehry [53]. Reference 3 has the drawn pattern not supporting the seating area, which is purposely designed to be structurally inefficient. Comparing these three reference designs, it is clearly seen that reference 1 is a performance-driven design, and references 2–3 are preference-driven designs, as $C = 29,340.694$ N mm, 516,371.303 N mm, and 840,141.598 for references 1–3, respectively. Note that references 2–3 include preferred patterns hoping to occur in the child designs.

This example uses two different strategies to create child designs, including (1) purely adjusting the drawing weights (see Figs. 11(b)–(c)), and (2) combining the drawing system with the scoring system in two generations of subsequent topology optimization (see Figs. 11(d)–(e)). In (1), the first generation of child designs (see Fig. 11(b)) are obtained with $\lambda_e = 1$ and $\lambda_d = 0.5$, aiming to achieve improved structural performance with a small distortion of the drawn pattern. Interestingly, it can be clearly seen that all four child designs have successfully preserved the drawn pattern with additional members added to enhance the structural performance. They have $g = 7$, and their C are significantly reduced, where $\Delta C = 0.12$, 0.13, 0.12, and 0.13 for solutions A–D, respectively. As shown in Fig. 11(c), the drawn pattern can be largely distorted if a smaller λ_d is used (i.e., 0.22). It can be seen that this generation of child designs has obtained different interesting shapes; $(\Delta g, P) = (6, 0.76)$, $(2, 0.72)$, $(3, 0.79)$, and $(0, 0.84)$ for solutions A–D, respectively. With this small adjustment of λ_d, the structural performance can be further improved; the best child design, solution A, has $\Delta C = 0.08$.

In (2), the first generation of child designs (see Fig. 11(d)) are created using $\lambda_e = 1$, $\lambda_s = 0$, and $\lambda_d = 0.75$. It can be seen that extra structural members are added to the drawn pattern, resulting in significantly enhanced structural performance; $\Delta C = 0.10$, 0.12, 0.11, and 0.08 for solutions A–D, respectively. Although this parameter setting allows the key geometric features of the drawn pattern to be preserved in the child designs, the four generated topologies are slightly different (see their Δg and P). Furthermore, the first generation of child designs can be scored to obtain better structural performance and design diversity, as shown in Fig. 11(e). Here, $S = -5$, -4, -2, and 5 for solutions

A–D of Fig. 11(d), respectively, meaning solution D is the only preferred design. Interestingly, it can be seen that the new child designs (see Fig. 11(e)) undertake the key geometric features of solution D of Fig. 11(d) and have achieved improved structural performance, where $\Delta C = 0.05$ (new solution A), 0.06 (new solutions B–C), and 0.07 (new solution D) are all smaller than 0.08 (previous solution D).

It is worth pointing out that all child designs (see Figs. 11(b)–(e)) have different shapes to reference 1 and with a dramatic performance loss. However, these child designs are considered more useful in practical applications, as they fulfill design requirements based on subjective preferences while maintaining a high level of structural efficiency. This example clearly demonstrates that structural performance is not the only consideration in determining a structural design; creative ideas to improve the aesthetic quality and achieve other design requirements are also valuable considerations.

6. Discussion

The proposed SP-BESO method is demonstrated to effectively obtain topologically different and structurally efficient solutions considering subjective preferences. There are many possible extensions of the proposed SP-BESO method, attributed to its simplicity of using the weighting method to penalize the sensitivity numbers. First, the proposed subjective scoring and drawing weights can be readily integrated into other topology optimization methods, such as the well-known SIMP and level-set methods. Specifically, these weights are scalar fields, which can be introduced to alter the sensitivity numbers, thereby affecting the formation of final structural topologies. In doing so, some inherent limitations of the underlying BESO method due to the use of discrete design variables may be avoided. It can be understood that such possible extensions with continuous design variables sacrifice the advantages of the BESO method (e.g., simplicity) in exchange for the capability of handling mathematically more complex structural design problems, such as multi-objective optimization problems. However, further study is needed to develop such possible extensions.

Second, it should be noted that the proposed SP-BESO method is currently limited to compliance minimization problems. Compliance (i.e., the inverse measure of stiffness) is a global measure of the structure, which has been widely used as the objective function in the literature to design stiff structures. However, for certain structural design problems, the overall stiffness of the structure may be less important, as the designers could be more concerned about the local performance, such as local displacement, stress, and buckling. There is potential to extend the proposed SP-BESO method to other structural optimization problems considering the optimization of local performance while ensuring subjective preferences. This is mathematically possible but remains unexplored. Besides, using the proposed drawing system, a slight change in the structural topology may significantly affect the local structural performance. Therefore, future research is required to consider different design objectives than compliance.

Finally, it is highly desirable to extend the proposed SP-BESO method to 3D structural design problems for more realistic practical applications. However, three technical challenges need to be solved to achieve this. First, it may be difficult for inexperienced designers to observe and evaluate 3D structures, which requires strong spatial awareness skills to look at many 3D details. Second, the proposed drawing system is difficult to operate in 3D space, meaning concisely and accurately interacting with 3D structures to include specific subjective preferences can be a complex task. Third, subjective interventions in 3D topology optimization may lead to more significant performance loss than in 2D cases due to an extremely high degree of design freedom; a slight modification of 3D structures can easily be far from the optimum and significantly affect the structural performance. These three technical challenges will be closely studied in future work, aiming to develop a practically useful 3D topology optimization software based on SP-BESO and make it available to the end-users in an easy, reliable, efficient, and inexpensive form.

7. Conclusion

This study presents a new topology optimization method, bi-directional evolutionary structural optimization with subjective preference (SP-BESO), by introducing subjective scoring and drawing systems into the structural optimization formulation. The proposed SP-BESO method is developed based on the conventional soft-kill BESO method. It converts the given scores and drawings as weights to penalize the elemental sensitivity numbers, thereby changing the relative ranking of sensitivity numbers, resulting in diverse, novel, competitive structural topologies with subjective preferences. Key findings of this study include: (1) parent designs can be imparted with low and high scores to obtain child designs with different and similar shapes, respectively, and (2) specifying a drawn pattern in topology optimization allows users to directly put their creative ideas into structural designs.

A series of examples are tested using the iBESO software [42] that is developed based on the proposed SP-BESO method. It is found that the combination of parameters used in both scoring and drawing systems controls the influence of subjective preferences in topology optimization so that the final structural topologies can be performance-driven or preference-driven. Moreover, this paper demonstrates that combined scoring and drawing strategies can be effectively adopted for practical applications to create desired structural designs. Although structural topologies obtained considering subjective preferences may have lower structural performance, they may be more useful in practical applications, as they consider other design requirements while maintaining a high level of structural efficiency. Future research may consider extending the proposed SP-BESO method to 3D structural design problems, thereby enabling the development of a wide range of efficient 3D structures considering subjective preferences.

Declaration of competing interest

The authors declare that they have no known competing financial interests or personal relationships that could have appeared to influence the work reported in this paper.

Data availability

Data will be made available on request. The iBESO software can be downloaded from: https://doi.org/10.25439/rmt.22560256.v1.

Acknowledgments

The authors gratefully acknowledge the financial support provided by the Australian Research Council (FL190100014). The authors would like to thank Professor Roland Snooks, Dr. Minghao Bi, Yulin Xiong, Yunzhen He, Dr. Xin Yan, Tao Xu, and Ahmed Abdelaal for their helpful advice on various technical issues examined in this paper.

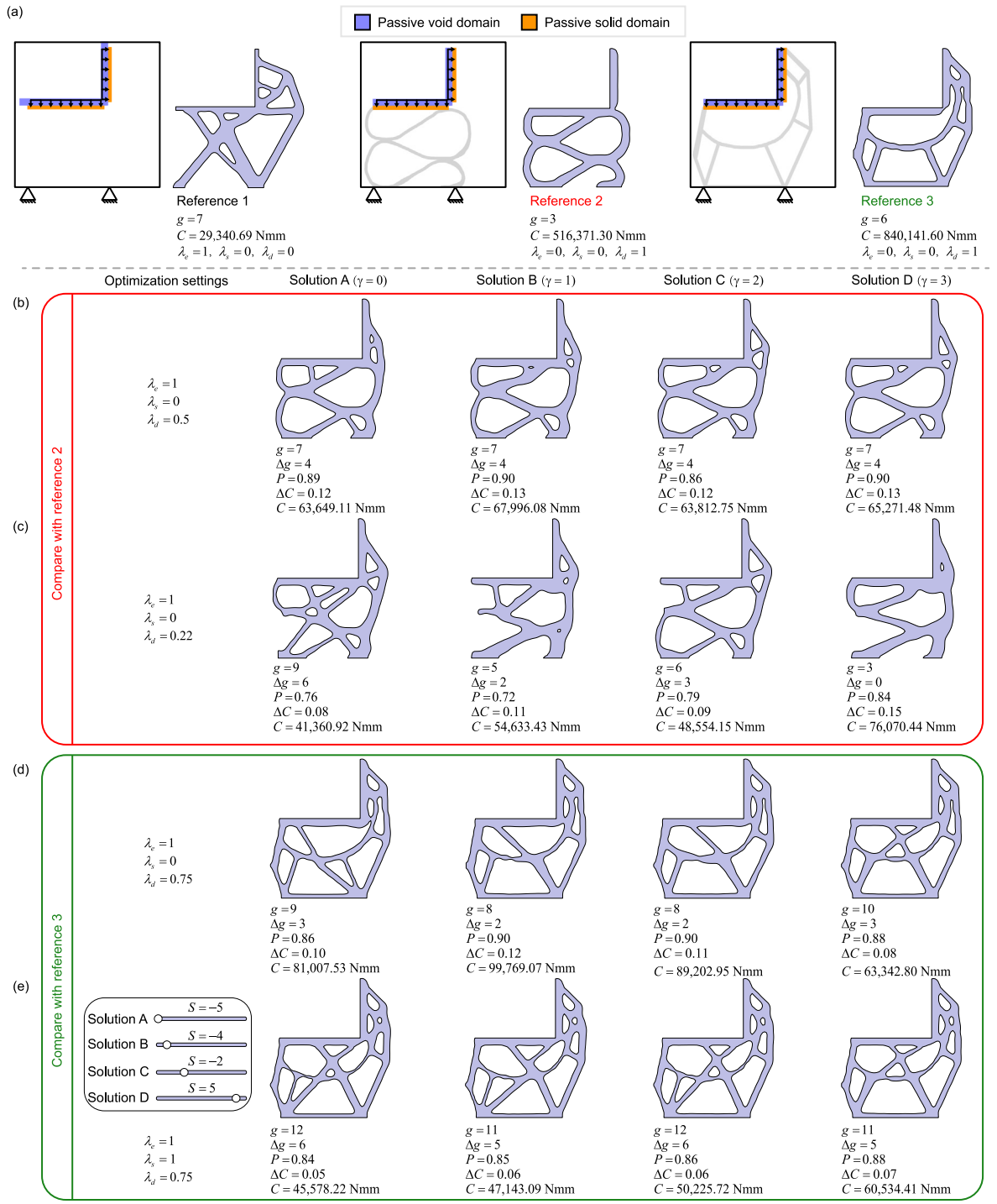

Fig. 11. 2D chair example: (a) reference 1 is the soft-kill BESO result, references 2–3 are obtained using different drawn patterns in SP-BESO; (b) child designs based on reference 2 ($\lambda_d = 0.5$); (c) child designs based on reference 2 ($\lambda_d = 0.22$); (d) child designs based on reference 3 ($\lambda_d = 0.75$); (e) scoring the last generation to generate new child designs. (For interpretation of the references to color in this figure legend, the reader is referred to the web version of this article.)

Appendix. Brush tool

The brush tool supports users in drawing patterns by clicking or swiping on the texture. For each click, a circular stroke is created on the mouse click position. Inspired by the famous image design tool, Adobe Photoshop, three stroke parameters are defined to create a rich drawing effect, including the radius, R, the hardness, H, and the opacity, O, of the stroke. Note that H and O are parameters ranging from 0% to 100%, which determines the sharpness of the stroke edge and the color of the stroke, respectively (see Fig. A.12(a)).

Fig. A.12(b) shows a point P in a stroke, its color can be calculated by

$$c'_P = \begin{cases} 1 - O, & \text{if } D \le RH \\ c_P + (1 - O)\dfrac{D - RH}{R(1 - H)}, & \text{if } D > RH \end{cases} \tag{A.1}$$

where c_P and c'_P represent the current color and the updated color of P on the texture, respectively. D is the distance between P and

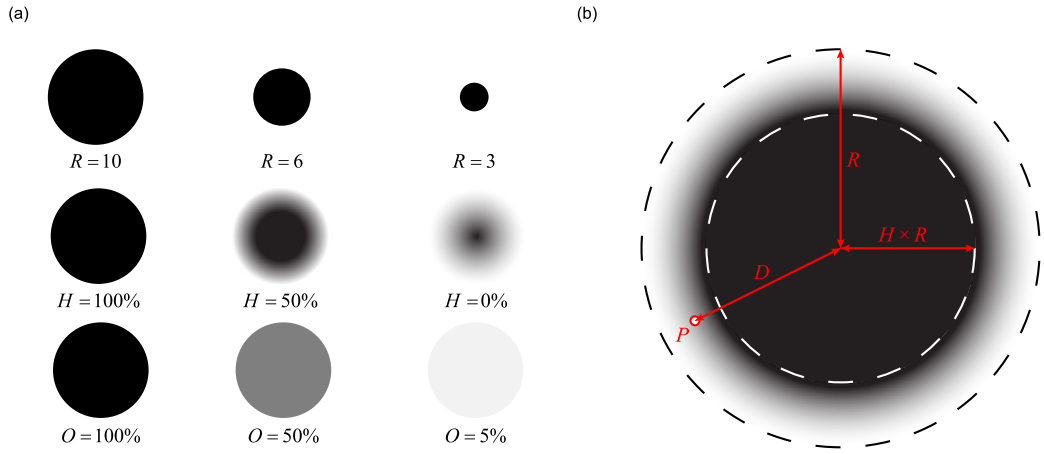

Fig. A.12. Brush stroke: (a) the effect of using different brush parameters; (b) the explanatory diagram of a stroke. (For interpretation of the references to color in this figure legend, the reader is referred to the web version of this article.)

the center of the stroke. Note that a new stoke may overlap the existing stoke, which requires c'_P to be further modified by

$$c''_P = \begin{cases} 1 - O, & if\ c'_P \geq 1 - O \\ c'_P, & if\ c'_P < 1 - O \end{cases} \tag{A.2}$$

where c''_P is the final color of P. In this way, creating strokes at a high frequency when swiping the mouse can simulate the effect of manual drawing [46].

References

[1] Bendsøe MP, Kikuchi N. Generating optimal topologies in structural design using a homogenization method. Comput Methods Appl Mech Engrg 1988;71:197–224. http://dx.doi.org/10.1016/0045-7825(88)90086-2.

[2] Bendsøe MP, Sigmund O. Topology optimization: theory, methods, and applications. Berlin: Springer; 2004.

[3] Aage N, Amir O, Clausen A, Hadar L, Maier D, Søndergaard A. Advanced topology optimization methods for conceptual architectural design. In: Advances in architectural geometry 2014. Cham: Springer; 2015, p. 159–79. http://dx.doi.org/10.1007/978-3-319-11418-7_11.

[4] Xie YM, Zuo ZH, Huang X, Tang JW, Zhao B, Felicetti P. Architecture and urban design through evolutionary structural optimisation algorithms. In: Proceedings of the international symposium on algorithmic design for architecture and urban design. Tokyo. 2011.

[5] Cui C, Ohmori H, Sasaki M. Computational morphogenesis of 3D structures by extended ESO method. J Int Assoc Shell Spatial Struct 2003;44:51–61.

[6] Lee TU, Xie YM. Simultaneously optimizing supports and topology in structural design. Finite Elem Anal Des 2021;197:103633. http://dx.doi.org/10.1016/j.finel.2021.103633.

[7] Ma J, Li Z, Zhao ZL, Xie YM. Creating novel furniture through topology optimization and advanced manufacturing. Rapid Prototyp J 2021;27:1749–58. http://dx.doi.org/10.1108/RPJ-03-2021-0047.

[8] Bhooshan V, Fuchs M, Bhooshan S. 3D-printing, topology optimization and statistical learning: a case study. In: Symposium on simulation for architecture and urban design. Toronto. 2017, p. 1–8. http://dx.doi.org/10.22360/simaud.2017.simaud.012.

[9] Bi M, Tran P, Xie YM. Topology optimization of 3D continuum structures under geometric self-supporting constraint. Addit Manuf 2022;36:101422. http://dx.doi.org/10.1016/j.addma.2020.101422.

[10] Xiong Y, Yao S, Zhao ZL, Xie YM. A new approach to eliminating enclosed voids in topology optimization for additive manufacturing. Addit Manuf 2020;32:101006. http://dx.doi.org/10.1016/j.addma.2019.101006.

[11] Bi M, Xia L, Tran P, Li Z, Wan Q, Wang L, Shen W, Ma G, Xie YM. Continuous contour-zigzag hybrid toolpath for large format additive manufacturing. Addit Manuf 2022;55:102822. http://dx.doi.org/10.1016/j.addma.2022.102822.

[12] Bi M, Xia L, Tran P, Ma G, Xie YM. Topology optimization for 3D concrete printing with various manufacturing constraints. Addit Manuf 2022;57:102982. http://dx.doi.org/10.1016/j.addma.2022.102982.

[13] Querin OM, Steven GP, Xie YM. Evolutionary structural optimisation (ESO) using a bidirectional algorithm. Eng Comput 1998;15:1031–48. http://dx.doi.org/10.1108/02644409810244129.

[14] Huang X, Xie YM. Convergent and mesh-independent solutions for the bidirectional evolutionary structural optimization method. Finite Elem Anal Des 2007;43:1039–49. http://dx.doi.org/10.1016/j.finel.2007.06.006.

[15] Huang X, Xie YM. Evolutionary topology optimization of continuum structures: methods and applications. Chichester: John Wiley & Sons; 2010.

[16] Ghabraie K. An improved soft-kill BESO algorithm for optimal distribution of single or multiple material phases. Struct Multidisc Optim 2015;52:773–90. http://dx.doi.org/10.1007/s00158-015-1268-2.

[17] Xie YM. Generalized topology optimization for architectural design. Archit Intell 2022;1:1–11. http://dx.doi.org/10.1007/s44223-022-00003-y.

[18] Loos S, Wolk Svd, Graaf Nd, Hekkert P, Wu J. Towards intentional aesthetics within topology optimization by applying the principle of unity-in-variety. Struct Multidiscip Optim 2022;65. http://dx.doi.org/10.1007/s00158-022-03288-9.

[19] Xie YM, Yang K, He Y, Zhao ZL, Cai K. How to obtain diverse and efficient structural designs through topology optimization. In: Proceedings of IASS annual symposia, international association for shell and spatial structures. IASS, 2019, p. 1977–84.

[20] He Y, Cai K, Zhao ZL, Xie YM. Stochastic approaches to generating diverse and competitive structural designs in topology optimization. Finite Elem Anal Des 2020;173:103399. http://dx.doi.org/10.1016/j.finel.2020.103399.

[21] Yang K, Zhao ZL, He Y, Zhou S, Zhou Q, Huang W, Xie YM. Simple and effective strategies for achieving diverse and competitive structural designs. Extreme Mech Lett 2019;30:100481. http://dx.doi.org/10.1016/j.eml.2019.100481.

[22] Lee TU, Xie YM. Optimizing load locations and directions in structural design. Finite Elem Anal Des 2022;209:103811. http://dx.doi.org/10.1016/j.finel.2022.103811.

[23] Wang B, Zhou Y, Zhou Y, Xu S, Niu B. Diverse competitive design for topology optimization. Struct Multidisc Optim 2018;57:891–902. http://dx.doi.org/10.1007/s00158-017-1762-9.

[24] Zhao ZL, Zhou S, Cai K, Xie YM. A direct approach to controlling the topology in structural optimization. Comput Struct 2020;227:106141. http://dx.doi.org/10.1016/j.compstruc.2019.106141.

[25] Yan X, Bao D, Zhou Y, Xie YM, Cui T. Detail control strategies for topology optimization in architectural design and development. Front Archit Res 2022;11:340–56. http://dx.doi.org/10.1016/j.foar.2021.11.001.

[26] He Y, Zhao ZL, Cai K, Kirby J, Xiong Y, Xie YM. A thinning algorithm based approach to controlling structural complexity in topology optimization. Finite Elem Anal Des 2022;207:103779. http://dx.doi.org/10.1016/j.finel.2022.103779.

[27] Davis D. Generative design is doomed to fail. 2022, https://www.danieldavis.com/generative-design-doomed-to-fail. [accessed 28 September 2022].

[28] Shi X, Yang W. Performance-driven architectural design and optimization technique from a perspective of architects. Autom Constr 2013;32:125–35. http://dx.doi.org/10.1016/j.autcon.2013.01.015.

[29] Canestrino G. On the influence of evolutionary algorithm (EA) optimization in architectural design: a reflection through an architectural evelope's shadowing system design. In: Proceedings of the 9th international conference of the arab society for computer aided architectural design, Cairo. 2021, p. 397–406.

[30] Schling E, Wang H, Hoyer S, Pottmann H. Designing asymptotic geodesic hybrid gridshells. Comput Aided Des 2022;152:103378. http://dx.doi.org/10.1016/j.cad.2022.103378.

[31] Zheng NN, Liu ZY, Ren PJ, Ma YQ, Chen ST, Yu SY, Xue JR, Chen BD, Wang FY. Hybrid-augmented intelligence: collaboration and cognition. Front Inf Technol Electron Eng 2017;18:153–79. http://dx.doi.org/10.1631/FITEE.1700053.
[32] Lidwell W, Holden K, Butler J. Universal principles of design, revised and updated: 125 ways to enhance usability, influence perception, increase appeal, make better design decisions, and teach through design. Rockport Pub; 2010.
[33] Li Y, Lai Y, Lu G, Yan F, Wei P, Xie YM. Innovative design of long-span steel–concrete composite bridge using multi-material topology optimization. Eng Struct 2022;269:114838. http://dx.doi.org/10.1016/j.engstruct.2022.114838.
[34] Takagi H. Interactive evolutionary computation: fusion of the capabilities of EC optimization and human evaluation. In: Proceedings of the IEEE. 2001, p. 1275–96. http://dx.doi.org/10.1109/5.949485.
[35] Cui J, Tang M. Integrating shape grammars into a generative system for Zhuang ethnic embroidery design exploration. Comput Aided Des 2013;45:591–604. http://dx.doi.org/10.1016/j.cad.2012.08.002.
[36] Mueller CT, Ochsendorf JA. Combining structural performance and designer preferences in evolutionary design space exploration. Autom Constr 2015;52:70–82. http://dx.doi.org/10.1016/j.autcon.2015.02.011.
[37] Yan X, Xiong Y, Bao D, Xie YM, Peng X. A multi-volume constraint approach to diverse form designs from topology optimization. Eng Struct 2023;279:115525. http://dx.doi.org/10.1016/j.engstruct.2022.115525.
[38] Sigmund O, Petersson J. Numerical instabilities in topology optimization: a survey on procedures dealing with checkerboards, mesh-dependencies and local minima. Struct Optim 1998;16:68–75. http://dx.doi.org/10.1007/BF01214002.
[39] Zuo ZH, Xie YM. A simple and compact python code for complex 3D topology optimization. Adv Eng Softw 2015;85:1–11. http://dx.doi.org/10.1016/j.advengsoft.2015.02.006.
[40] Huang W, Zheng H. Architectural drawings recognition and generation through machine learning. In: Proceedings of the 38th annual conference of the association for computer aided design in architecture (ACADIA). Mexico. 2018, p. 156–65. http://dx.doi.org/10.52842/conf.acadia.2018.156.
[41] Kirkland EJ. Bilinear interpolation. In: Advanced computing in electron microscopy. Boston: Springer; 2010, p. 261—63. http://dx.doi.org/10.1007/978-1-4419-6533-2_12.
[42] Li Z, Lee TU, Xie YM. iBESO: an interactive topology optimization design tool. 2023, http://dx.doi.org/10.25439/rmt.22560256.v1.
[43] Andreassen E, Clausen A, Schevenels M, Lazarov BS, Sigmund O. Efficient topology optimization in MATLAB using 88 lines of code. Struct Multidisc Optim 2011;43:1–16. http://dx.doi.org/10.1007/s00158-010-0594-7.
[44] Ferrari F, Sigmund O. A new generation 99 line matlab code for compliance topology optimization and its extension to 3D. Struct Multidisc Optim 2020;62:2211–28. http://dx.doi.org/10.1007/s00158-020-02629-w.
[45] Li Z, Lee TU, Yao Y, Xie YM. Smoothing topology optimization results using pre-built lookup tables. Adv Eng Softw 2022;173:103204. http://dx.doi.org/10.1016/j.advengsoft.2022.103204.
[46] Finnell A. How to implement a basic bitmap brush. 2007, https://losingfight.com/blog/2007/08/18/how-to-implement-a-basic-bitmap-brush/. [accessed 28 September 2022].
[47] Giachetti A. Matching techniques to compute image motion. Image Vis Comput 2000;18:247–60. http://dx.doi.org/10.1016/S0262-8856(99)00018-9.
[48] Zhang W, Liu Y, Wei P, Zhu Y, Guo X. Explicit control of structural complexity in topology optimization. Comput Methods Appl Mech Engrg 2017;324:149–69. http://dx.doi.org/10.1016/j.cma.2017.05.026.
[49] Han H, Guo Y, Chen S, Liu Z. Topological constraints in 2D structural topology optimization. Struct Multidiscip Optim 2021;63:39–58. http://dx.doi.org/10.1007/s00158-020-02771-5.
[50] Hatcher A. Algebraic topology. Cambridge University Press; 2002.
[51] Crossley MD. Essential topology. Springer Science & Business Media; 2006.
[52] Clausen A, Aage N, Sigmund O. Topology optimization with flexible void area. Struct Multidisc Optim 2014;50:927–43. http://dx.doi.org/10.1007/s00158-014-1109-8.
[53] Martin H. The story behind Frank Gehry's iconic wiggle design. 2018, https://www.architecturaldigest.com/story/the-story-behind-frank-gehrys-iconic-wiggle-design. [accessed 28 September 2022].